What can a machine learn from a single first-principles calculation?

Nicholas Rajen[1] and Sinisa Coh[1,2,*]

[1] *Materials Science and Engineering, University of California Riverside, Riverside, CA 92521, USA*
[2] *Mechanical Engineering, University of California Riverside, Riverside, CA 92521, USA*

(Dated: June 7, 2017)

We extract an energy scale X from electron orbitals $\Psi_{n\mathbf{k}}$ and energies $E_{n\mathbf{k}}$ in ABO_3 perovskite in its high-symmetry cubic state. Even though X was calculated in the high-symmetry state we show that its value dictates material's true low-symmetry ground state structure. We propose using concealed variables such as X not only for material structure prediction algorithms but also for high-throughput approaches.

PACS numbers: 61.50.-f,71.15.-m

There is a growing need for machines to learn about matter from results of a large set of first-principles computer calculations. However, a single such calculation produces $\sim 10^6$–10^9 bits of information and it is unclear which of those bits should machine learn from.[1, 2] Therefore machines typically set aside most of these bits — such as bits describing electron orbitals Ψ — and try to learn from the simplest calculated quantities such as the total energy E^{tot} or similar.

One such example where machines are learning from E^{tot} are methods used for predicting positions of atoms in a yet unsynthesized material. These methods look for a set of atom positions ξ that minimize the total energy $E^{\text{tot}}(\xi)$ of the material. Total energy can be computed reasonably accurately from first-principles approaches such as those based on the density functional theory.[3, 4] However, minimization of $E^{\text{tot}}(\xi)$ still remains an unsolved problem as ξ is a vector in a very highly dimensional space (it has $\approx 3N$ dimensions and N is a number of atoms in the material). Nevertheless, this problem can be addressed heuristically using machine learning techniques such as evolutionary algorithms[5] or particle swarm optimization.[6] Quite broadly speaking these methods first use E^{tot} calculated for a wide range of different candidate structures $\xi_1, \xi_2, ...\xi_n$, but the same chemical composition, to learn about the underlying interactions in that material. Next, given this knowledge, the machine makes an informed guess for the next structure ξ_{n+1} and the process repeats until an optimal structure is found.

Need for a machine to learn in the context of materials science is also relevant for the so-called high-throughput approaches such as the materials project,[7] the aflow,[8] or the oqmd[9] materials databases. While in the structure prediction problem one considers a single chemical composition at the time, in the high-throughput approach one wishes to learn about materials with a wide range of chemical compositions. Since these databases contain information for $\sim 10^5$–10^6 materials their total information content is $\sim 10^{14}$–10^{15} bits.

In this paper we do not focus on what machines can learn from E^{tot} or how should they learn from E^{tot}. Instead, we wish to find a variable X from which learning could be more efficient. For concreteness, we work for now in the context of structure prediction algorithms, but the same ideas likely extend to high-throughput approaches as well.

As a test case, we considered structures of ABO_3 perovskites as they are extensively studied, both experimentally and theoretically.[10] Some of these materials condense into a *polar* structure (with A and B displaced relative to O atoms) while others condense into a *tilted* structure (with rotated oxygen octahedra).[11–13] We now seek to find a variable X — to be computed in some way from the high-symmetry cubic state — that is correlated with whether the ground state structure of the material is polar or tilted. If such a variable can be found then it clearly has learning potential. As a comparison, the total energy does not have that learning potential as the cubic structure does not contain polar or tilt distortions. Therefore one can not compare total energy reduction of the polar distortion versus the tilt distortion. In fact, even if one estimated that energy reduction — say, by computing the second derivative of E^{tot} with respect to polar and tilt distortions (these are related to the so-called unstable phonon frequencies[14]) — one finds, somewhat paradoxically, that perovskites with larger energy reduction due to polar modes tend to have greater tendency for *tilted* structure.[12] One gets a correct preference for the ground state structure only by computing higher order derivatives in the Taylor expansion of the total energy E^{tot}.[15]

In addition to having (i) a learning potential, a useful variable X should also satisfy additional two criteria: (ii) X should be represented with as few numbers as possible, so that learning is as efficient as possible; (iii) X should be calculable automatically for a given material without (nearly) any input from the user, so that it can be used by a machine.

To satisfy the criterion (i) of having a learning potential, X should ideally be in some way derived from the fundamental variable of the problem. In the case of quantum mechanical descriptions of matter, the fundamental variable is the electron many-body wave function

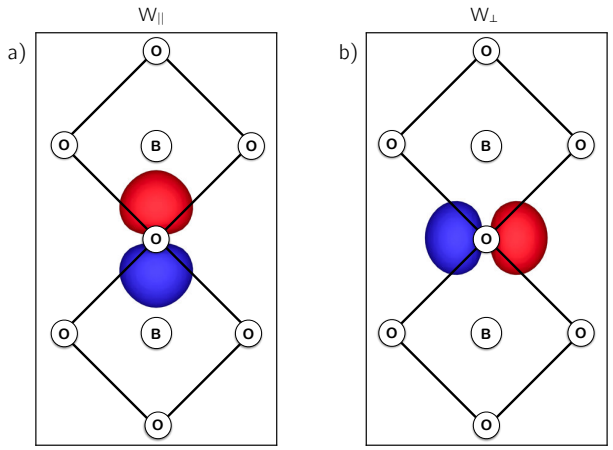

FIG. 1. Isosurfaces of two symmetry distinct Wannier functions $W_{\parallel}$ (panel a) and $W_{\perp}$ (panel b) in the case of $BaTiO_3$. Red and blue colors correspond to positive and negative sign.

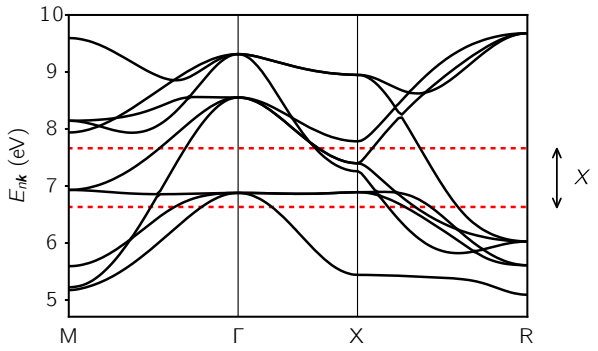

FIG. 2. Band structure of nine dominantly oxygen p-like bands in $SrTiO_3$. Two dashed red lines are indicating $\langle W_{\perp}|H|W_{\perp}\rangle$ (top red line) and $\langle W_{\parallel}|H|W_{\parallel}\rangle$ (bottom). Their difference (X) is denoted by a black arrow.

$\widetilde{\Psi}$. [We note in passing that the many-body wave function $\widetilde{\Psi}$ is formally not accessible in the commonly used Kohn-Sham[4] scheme for the density functional theory. Therefore we instead use here the so-called Kohn-Sham orbitals $\Psi_{n\boldsymbol{k}}$ (and corresponding energies $E_{n\boldsymbol{k}}$) as they are typically reasonably good approximations[16] of the quasi-electron and hole wave functions and energies (here n is a band index while $\boldsymbol{k}$ is a crystal momentum).]

Orbitals $\Psi_{n\boldsymbol{k}}$ themselves are not a good choice of X as they do not satisfy criterion (ii). Namely, even in the simplest calculations (say, cubic silicon), a machine needs $\sim 10^6$ bits to describe $\Psi_{n\boldsymbol{k}}$ reasonably accurately. As discussed later, we circumvent this difficulty by defining X in terms of the Wannier functions[17], as they provide a compact and faithful representation of $\Psi_{n\boldsymbol{k}}$. Wannier functions can be computed without user input[18] so our approach satisfies condition (iii) as well.

Quite surprisingly, we find that there is a unique energy scale X — extracted from cubic ABO_3 — that we find to be correlated with whether the ground state structure is polar or tilted. In particular, perovskites with X less than ~ 1 eV condense into a tilted state while those with X larger than ~ 1 eV condense into a polar state. This energy scale X (defined later) can intuitively be interpreted as oxygen bonding anisotropy, as it measures the difference in energy of bond perpendicular (π-bond) and parallel (σ-bond) to the B–O–B direction. Therefore, in a material with a highly anisotropic bond, energy is lowered by dimerizing the B–O–B triplet. In material with less anisotropy energy is lowered by bending the triplet. We note here that importance of local interactions in perovskites has been discussed earlier in Refs. [11, 19–22]. However, we are unaware of any other work in which density functional calculation of a high-symmetry perovskite alone can be used to infer its low-symmetry ground state structure.

We focus here for simplicity on insulating perovskites where both A and B atoms have nominally closed electronic shells. We identified twelve well-studied perovskites covering both polar and tilted ground states. Our calculations are based on a generalized gradient approximation[23] to the density functional theory and use the norm-conserving pseudopotentials[24, 25] within the quantum-espresso package.[26] In all cases we include the semi-core electrons into the calculation. We start by computing the structure of all twelve ABO_3 perovskites in an ideal high-symmetry state. The unit cell of the ideal perovskite contains one ABO_3 formula unit. The oxygen atoms form corner-sharing octahedra. The B atoms are in the center of those octahedra while A atoms are outside. This structure is indicated with black lines and circles in Fig. 1. Since all atoms are in the high-symmetry positions, the ideal perovskite structure is characterized by a single parameter: cubic lattice parameter a. We determined a for each of the twelve studied perovskites by minimizing the total energy $E^{\rm tot}$ with respect to a. For the structural calculation we used a 4x4x4 k-grid and we cutoff the plane wave basis at 130 Ry. The calculated numerical values of a for each case are given in the supplement.[27]

As described earlier, our goal is now to use Kohn-Sham orbitals $\Psi_{n\boldsymbol{k}}$ and energies $E_{n\boldsymbol{k}}$ to infer the preference of the high-symmetry structure for either polar or tilted structural distortion. For simplicity we will focus only on electron bands with a dominant oxygen p-like character. While there is nothing preventing us from studying other bands as well, oxygen p-like bands are the most dispersive in metal-oxide perovskites and thus should contain most information about the inter-atomic interactions in the material. Since there are three oxygen atoms in the unit cell, we have in total nine oxygen p-like bands. These bands in the representative case of $SrTiO_3$ are shown in Fig. 2.

For convenience we convert calculated $\Psi_{n\boldsymbol{k}}$ into a ba-

sis of maximally localized Wannier functions[17, 28, 29] W_n. This significantly simplifies our analysis as Wannier functions are typically strongly localized on a single atom[29, 30] and are therefore more convenient descriptors of the chemical environment of a material. Given a set of extended periodic orbitals $\Psi_{n\boldsymbol{k}}$ Wannier functions W_n are defined as,

$$W_n(\boldsymbol{r}) = \frac{1}{N_{\boldsymbol{k}}} \sum_k U_{nm\boldsymbol{k}} \Psi_{m\boldsymbol{k}}(\boldsymbol{r}) \tag{1}$$

where $N_{\boldsymbol{k}}$ is a total number of k-points. While unitary matrices $U_{nm\boldsymbol{k}}$ are in principle arbitrary, in the case of maximally localized Wannier functions they are chosen so that the resulting function $W_n(\boldsymbol{r})$ is as localized in real space as possible.[29]

We stress out that basis change in Eq. (1) is exact in the sense that the vector space spanned by W_n (and its periodic images) is the same as space spanned by $\Psi_{m\boldsymbol{k}}$. However, W_n is a more convenient object to study than $\Psi_{n\boldsymbol{k}}$ since a single function W_n contains the same information as an entire band of Bloch functions $\Psi_{n\boldsymbol{k}}$ (there is one function for each $\boldsymbol{k}$-point). Therefore any information contained in nine oxygen p-like bands is also contained in the corresponding nine Wannier functions. One of the Wannier functions, shown in Fig. 1 (a) and denoted by $W_\parallel$, corresponds to the atomic p-like function oriented along the B–O–B line (here B is the transition metal in ABO_3 perovskite that is in the center of the oxygen octahedron). The remaining two functions centered on the same oxygen atom are perpendicular to the B–O–B line [see Fig. 1 (b)].

Since Wannier functions are a compact representation of a band-structure, they are also a compact representation of quantum mechanical operators. For example, the Hamiltonian operator H can be represented in the Wannier basis as,

$$H_{nm\boldsymbol{R}} = \langle W_n | H | W_{m\boldsymbol{R}} \rangle \,. \tag{2}$$

Here $W_{m\boldsymbol{R}}$ is defined as W_m translated by a lattice vector $\boldsymbol{R}$,

$$W_{m\boldsymbol{R}}(\boldsymbol{r}) = W_m(\boldsymbol{r} - \boldsymbol{R}).$$

We calculated $H_{nm\boldsymbol{R}}$ for all twelve perovskites using Wannier90 package.[31] For this calculation we used relaxed lattice parameter a and sampled the Brillouin zone on a 6x6x6 grid.

We start by analyzing $H_{nm\boldsymbol{R}}$ when either $n \neq m$ or $\boldsymbol{R} \neq \boldsymbol{0}$. These terms are often referred to as hopping integrals. Since W_n are exponentially localized functions, hopping integral $H_{nm\boldsymbol{R}}$ is exponentially small when W_n and $W_{m\boldsymbol{R}}$ are far enough from each other in space. In the case of twelve compounds we studied we find that in all cases $|H_{nm\boldsymbol{R}}| < 0.2$ eV when W_n and $W_{m\boldsymbol{R}}$ are separated by more than one lattice spacing ($a \approx 4$–5 Å).[27]

TABLE I. Variable X calculated in a high-symmetry cubic state correlates well with the low-symmetry ground state structure. See main text for more detail.

Material	Variable X (eV)	Structure
$CaZrO_3$	0.47	tilted
$SrZrO_3$	0.57	tilted
$PbZrO_3$	0.70	tilted
$BaZrO_3$	0.76	tilted
$SrHfO_3$	0.76	tilted
$CaTiO_3$	0.91	tilted
$SrTiO_3$	1.03	polar/tilted
$PbTiO_3$	1.20	polar
$BaTiO_3$	1.25	polar
$NaNbO_3$	1.31	polar
$KNbO_3$	1.45	polar
$KTaO_3$	1.66	polar

The magnitude of the shorter distance hopping terms is up to $\sim$ 1.0 eV. Due to symmetry, there are only six distinct short-range hopping integrals. We label them as t_1 through t_6 and provide their numerical values in the supplement.

However, hopping integrals do not contribute directly to the integrated band energy $\int_{\mathrm{BZ}} E_{n\boldsymbol{k}} d\boldsymbol{k}$ and therefore they likely don't have the learning potential for determining ground state structure. One can easily show that for a single fully occupied band $\int_{\mathrm{BZ}} E_{n\boldsymbol{k}} d\boldsymbol{k}$ is independent of the hopping integral. This property also extends to the case of multiple bands. Of course, total energy E^{tot} in the Kohn-Sham framework does not depend only on $\int_{\mathrm{BZ}} E_{n\boldsymbol{k}} d\boldsymbol{k}$ but also on additional terms that are explicit functions of electron density $n(\boldsymbol{r})$. However, density can be computed from the Wannier function as $n(\boldsymbol{r}) = \sum_{n\boldsymbol{R}} |W_n(\boldsymbol{r})|^2$. Therefore, in some classes of materials it is possible that one would have to include a descriptor for the shape of the Wannier function in order to learn about the material structure. However, we find that not to be the case for perovskites as we find that shape of the oxygen Wannier function is nearly constant among materials we studied.

Now we turn to $H_{nm\boldsymbol{R}}$ for remaining cases when both $n = m$ and $\boldsymbol{R} = \boldsymbol{0}$. The corresponding $H_{nn\boldsymbol{0}}$ is usually referred to as the onsite energy of the n-th Wannier function. The absolute value of onsite energy is ill-defined for a periodic solid as one can change its value by adding an arbitrary constant C to the Hamiltonian of the periodic solid: $H \to H + C$. However, changing H to $H + C$ changes onsite energies of all nine Wannier functions by the same amount. Therefore, even though absolute values are ill-defined, the differences of onsite energies,

$$H_{nn\boldsymbol{0}} - H_{mm\boldsymbol{0}} \tag{3}$$

are well defined.

Clearly, the difference of onsite energies $H_{nn\mathbf{0}} - H_{mm\mathbf{0}}$ is zero if n and m correspond to two Wannier functions related to each other by a crystal symmetry (such as rotation or inversion). Since the symmetry of ideal perovskite structure is so high, the only non-zero term $H_{nn\mathbf{0}} - H_{mm\mathbf{0}}$ is the one where n corresponds to $W_\perp$ and m to $W_\parallel$ (or vice versa). This difference we will denote as,

$$X = \langle W_\perp|H|W_\perp\rangle - \langle W_\parallel|H|W_\parallel\rangle . \quad (4)$$

Figure 2 shows a complex of nine oxygen p-like electron bands (black lines) in $SrTiO_3$ along with calculated $\langle W_\perp|H|W_\perp\rangle$ and $\langle W_\parallel|H|W_\parallel\rangle$ (dashed red). The black arrow indicates their difference (X). The numerical value of X for all materials we studied is provided in Tab. I. As can be seen from the table, X is positive in all cases so $W_\perp$ is less hybridized with neighboring A and B atoms than $W_\parallel$. This is expected as $W_\parallel$ points towards the first neighboring B ion so it can form a stronger bond. The calculated values of X across twelve materials range from 0.47 eV to 1.66 eV.

We stress here that the energy scale X can not be inferred from the electron band-energies $E_{n\boldsymbol{k}}$ alone. Instead, one also needs wave functions $\Psi_{n\boldsymbol{k}}$. In addition, X is gauge-dependent as a different choice of relative phases of wave functions will lead to a different Wannier function and thus different X. For example, one can show that a simple unitary rotation that rotates $W_\parallel$ and $W_\perp$ will produce two Wannier function with the difference in onsite energy having any value between $+X$ and $-X$, including zero.

Since we expect t_1,...t_6 not to be important for the structure, the only relevant energy scale in the problem remains X. Indeed, we find that X is well correlated with the preferred low-symmetry structure of ABO_3 perovskites as shown in Tab. I. In particular, we find that materials with X larger than ~ 1 eV have a polar structure while those with X less than ~ 1 eV have a tilted structure. As can be seen from the Fig. 1 in the supplement[27] variables t_1,...t_6 do not show this correlation with the structural ground state, as expected.

We now discuss structures of these perovskites in more detail, as not all of them can be described just by being tilted or polar. $CaZrO_3$, $SrZrO_3$, $SrHfO_3$, and $CaTiO_3$ are well-established to form a tilted structure with a Pbnm space group (62) and tilt pattern ($a^-a^-c^+$) in the Glazer notation.[13] Structures of $PbZrO_3$ and $BaZrO_3$ are somewhat more involved. $PbZrO_3$ has antipolar distortion in an addition to tilts[32] while $BaZrO_3$ is shown computationally to have somewhat differently tilted structure ($a^-b^-c^-$) instead of ($a^-a^-c^+$).[33] As is well-known $SrTiO_3$ is an interesting case as it has nearly degenerate polar and tilted structures.[34] Regarding the structure of polar materials: $PbTiO_3$, $BaTiO_3$, and $KNbO_3$ are all well known to have relatively simple polar structures with small primitive unit cells.[15, 35] $KTaO_3$ is experimentally found to be an incipient ferroelectric, similar to $SrTiO_3$, but with polar microregions.[36, 37] First principles calculations performed on $KTaO_3$[38] find it to be on the verge of cubic–polar phase transition. We repeated those calculations with semi-core pseudopotentials and we find $KTaO_3$ to be polar. Finally, experimentally $NaNbO_3$ is found to have competing polar and anti-polar ground state.[39] First-principles calculations find a slight preference for the polar over the antipolar structure.[39, 40] Therefore, in conclusion, variable X is very well correlated with the preferred ground state for most materials (9 out of 12). For remaining (3) materials trends are captured correctly, but one would need to do a more detailed analysis to resolve the subtleties of their ground state structures. One possibility is to consider onsite-energies of oxygen s-like bands or bands dominated by electrons on A or B atoms.

While X is a unique relevant energy scale for cubic ABO_3 perovskites in other material classes relevant variable X might correspond to more than one number. For example, this will happen in materials where atoms occupy either lower symmetry Wyckoff orbits, or the same atom occupies more than one Wyckoff orbit. Furthermore, we expect that for materials made of atoms that form different bonding environments (say sp^2 carbon in graphite versus sp^3 carbon in diamond) one would have to include in variable X also the shape of the Wannier function, as discussed earlier. This could be achieved for example by decomposing the Wannier function in the basis of atomic orbitals.[18, 41] Therefore, we expect that approach presented here for ABO_3 perovskites will extend to other classes of materials. In addition, we expect that this approach could be extended to high-throughput environments as well since X was blindly extracted from the fundamental variable in the problem ($\Psi_{n\boldsymbol{k}}$) without relying on chemical intuition. Finally, we expect that one could use this approach not only to characterize Hamiltonian operator H but also any other quantum-mechanical operator, such as electron-light interaction or electron-phonon interaction.[42]

* sinisacoh@gmail.com

[1] S. Curtarolo, G. L. W. Hart, M. B. Nardelli, N. Mingo, S. Sanvito, and O. Levy, Nat. Mater. **12**, 191 (2013).
[2] L. M. Ghiringhelli, J. Vybiral, S. V. Levchenko, C. Draxl, and M. Scheffler, Phys. Rev. Lett. **114**, 105503 (2015).
[3] P. Hohenberg and W. Kohn, Phys. Rev. **136**, B864 (1964).
[4] W. Kohn and L. J. Sham, Phys. Rev. **140**, A1133 (1965).
[5] A. O. Lyakhov, A. R. Oganov, H. T. Stokes, and Q. Zhu, Computer Physics Communications **184**, 1172 (2013).
[6] Y. Wang, J. Lv, L. Zhu, and Y. Ma, Computer Physics Communications **183**, 2063 (2012).
[7] A. Jain, G. Hautier, C. J. Moore, S. Ping Ong, C. C. Fischer, T. Mueller, K. A. Persson, and G. Ceder, Com-

putational Materials Science **50**, 2295 (2011).
[8] S. Curtarolo, W. Setyawan, S. Wang, J. Xue, K. Yang, R. H. Taylor, L. J. Nelson, G. L. Hart, S. Sanvito, M. Buongiorno-Nardelli, N. Mingo, and O. Levy, Computational Materials Science **58**, 227 (2012).
[9] J. E. Saal, S. Kirklin, M. Aykol, B. Meredig, and C. Wolverton, JOM **65**, 1501 (2013).
[10] R. J. D. Tilley, *Perovskites: structure-property relationships* (John Wiley and Sons, Ltd, 2016).
[11] P. M. Woodward, Acta Crystallogr. B **53**, 44 (1997).
[12] N. A. Benedek and C. J. Fennie, J. Phys. Chem. C **117**, 13339 (2013).
[13] A. M. Glazer, Acta Crystallographica Section B **28**, 3384 (1972).
[14] S. Baroni, S. de Gironcoli, A. Dal Corso, and P. Giannozzi, Rev. Mod. Phys. **73**, 515 (2001).
[15] R. D. King-Smith and D. Vanderbilt, Phys. Rev. B **49**, 5828 (1994).
[16] M. S. Hybertsen and S. G. Louie, Phys. Rev. B **34**, 5390 (1986).
[17] N. Marzari, A. A. Mostofi, J. R. Yates, I. Souza, and D. Vanderbilt, Rev. Mod. Phys. **84**, 1419 (2012).
[18] J. I. Mustafa, S. Coh, M. L. Cohen, and S. G. Louie, Phys. Rev. B **92**, 165134 (2015).
[19] R. E. Cohen, Nature **358**, 136 (1992).
[20] I. B. Bersuker, Ferroelectrics **164**, 75 (1995).
[21] M. H. Palmer, Journal of Molecular Structure **405**, 193 (1997).
[22] A. Koleyski and K. Tkacz-miech, Ferroelectrics **314**, 123 (2005).
[23] J. P. Perdew, K. Burke, and M. Ernzerhof, Phys. Rev. Lett. **77**, 3865 (1996).
[24] D. R. Hamann, Phys. Rev. B **88**, 085117 (2013).
[25] M. Schlipf and F. Gygi, Computer Physics Communications **196**, 36 (2015).
[26] P. Giannozzi *et al.*, Journal of Physics: Condensed Matter **21**, 395502 (2009).
[27] See supplementary information.
[28] G. H. Wannier, Phys. Rev. **52**, 191 (1937).
[29] N. Marzari and D. Vanderbilt, Phys. Rev. B **56**, 12847 (1997).
[30] C. Brouder, G. Panati, M. Calandra, C. Mourougane, and N. Marzari, Phys. Rev. Lett. **98**, 046402 (2007).
[31] A. A. Mostofi, J. R. Yates, Y.-S. Lee, I. Souza, D. Vanderbilt, and N. Marzari, Computer Physics Communications **178**, 685 (2008).
[32] D. J. Singh, Phys. Rev. B **52**, 12559 (1995).
[33] A. Bilić and J. D. Gale, Phys. Rev. B **79**, 174107 (2009).
[34] K. A. Müller and H. Burkard, Phys. Rev. B **19**, 3593 (1979).
[35] M. Posternak, R. Resta, and A. Baldereschi, Phys. Rev. B **50**, 8911 (1994).
[36] H. Uwe, K. B. Lyons, H. L. Carter, and P. A. Fleury, Phys. Rev. B **33**, 6436 (1986).
[37] O. Aktas, S. Crossley, M. A. Carpenter, and E. K. H. Salje, Phys. Rev. B **90**, 165309 (2014).
[38] A. R. Akbarzadeh, L. Bellaiche, K. Leung, J. Íñiguez, and D. Vanderbilt, Phys. Rev. B **70**, 054103 (2004).
[39] S. K. Mishra, N. Choudhury, S. L. Chaplot, P. S. R. Krishna, and R. Mittal, Phys. Rev. B **76**, 024110 (2007).
[40] R. Machado, M. Sepliarsky, and M. G. Stachiotti, Ferroelectrics **427**, 98 (2012).
[41] J. Bhattacharjee and U. V. Waghmare, Phys. Chem. Chem. Phys. **12**, 1564 (2010).
[42] F. Giustino, J. R. Yates, I. Souza, M. L. Cohen, and S. G. Louie, Phys. Rev. Lett. **98**, 047005 (2007).

Supplement for: "What can a machine learn from a single first-principles calculation?"

Nicholas Rajen[1] and Sinisa Coh[1,2]

[1]*Materials Science and Engineering, University of California Riverside, Riverside, CA 92521, USA*
[2]*Mechanical Engineering, University of California Riverside, Riverside, CA 92521, USA*

(Dated: June 7, 2017)

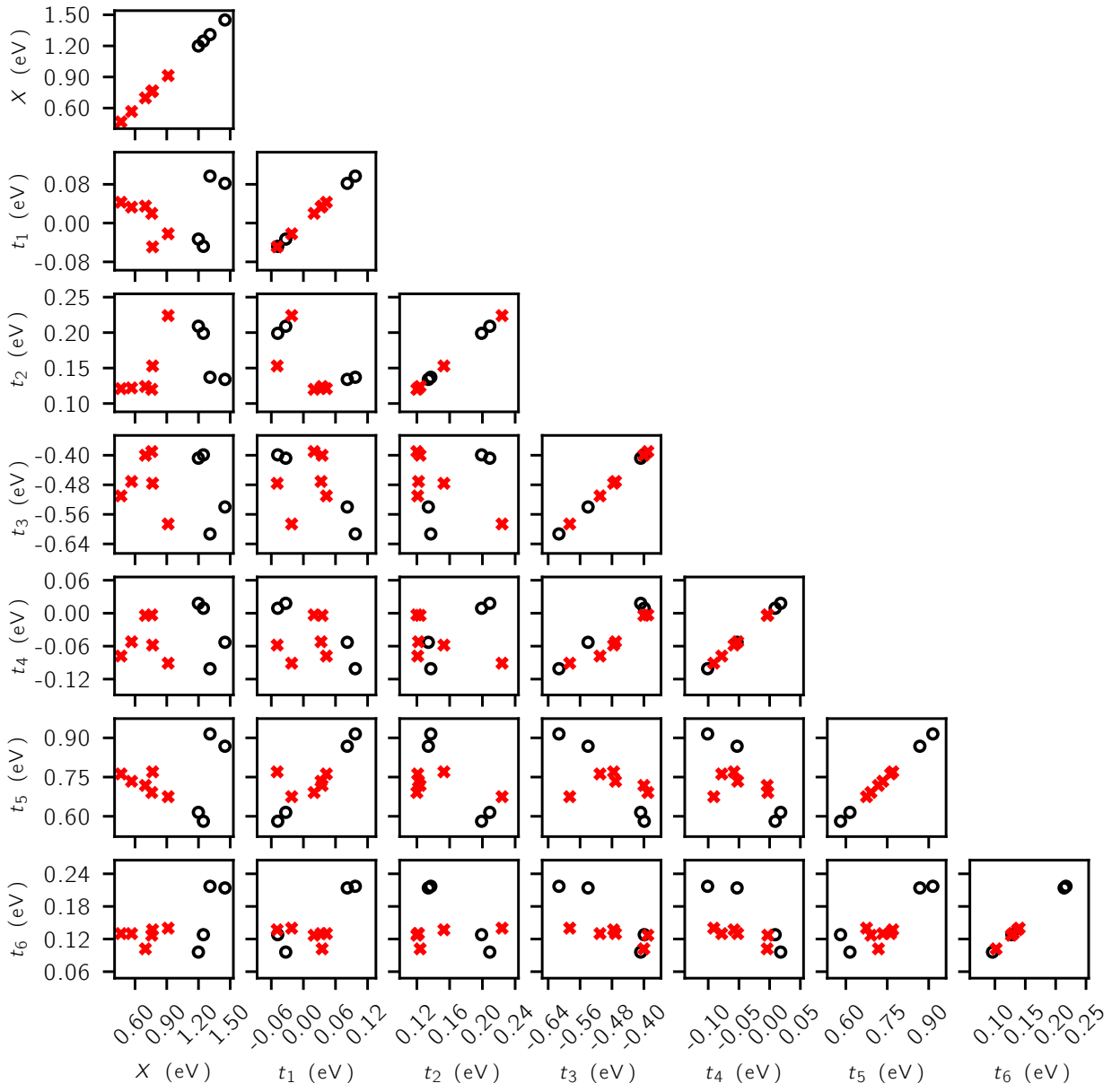

FIG. 1. Plots of all seven variables (X, t_1,...t_6) for all twelve materials we studied. Tilted materials are indicated with red crosses while polar with black circles. Clearly, X is correlated with the preference for a polar or a tilted structure, while t_1,...t_6 are not, as expected. See main text for more details.

TABLE I. Numerical values of calculated lattice parameter a, on-site energy difference X, and hopping integrals for all studied materials.

	a(Å)	X (eV)	t_1 (eV)	t_2 (eV)	t_3 (eV)	t_4 (eV)	t_5 (eV)	t_6 (eV)
$CaZrO_3$	4.136	0.467	0.043	0.121	-0.510	-0.078	0.762	0.130
$SrZrO_3$	4.169	0.567	0.033	0.122	-0.471	-0.052	0.734	0.130
$PbZrO_3$	4.186	0.698	0.035	0.124	-0.400	-0.004	0.718	0.102
$BaZrO_3$	4.227	0.758	0.020	0.120	-0.390	-0.003	0.691	0.127
$SrHfO_3$	4.148	0.766	-0.049	0.153	-0.476	-0.058	0.770	0.137
$CaTiO_3$	3.884	0.913	-0.022	0.224	-0.586	-0.091	0.675	0.140
$SrTiO_3$	3.937	1.030	-0.033	0.216	-0.522	-0.055	0.636	0.137
$PbTiO_3$	3.968	1.199	-0.033	0.209	-0.408	0.018	0.615	0.096
$BaTiO_3$	4.020	1.246	-0.048	0.199	-0.399	0.009	0.581	0.128
$NaNbO_3$	3.977	1.309	0.097	0.137	-0.613	-0.101	0.915	0.217
$KNbO_3$	4.027	1.450	0.082	0.134	-0.540	-0.053	0.868	0.214
$KTaO_3$	4.021	1.662	-0.007	0.153	-0.540	-0.058	0.909	0.211

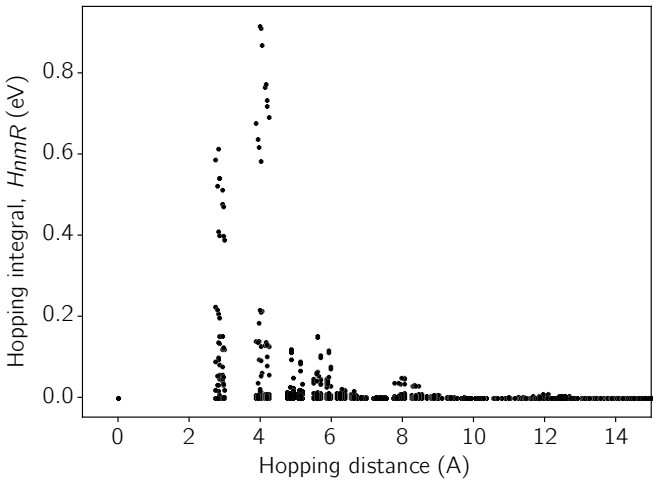

FIG. 2. The absolute value of all hopping integrals for all twelve materials we studied as a function of hopping distance. Hopping distance is defined as a distance from the center of n-th and m-th Wannier function. As one can see from the figure, hopping integrals quickly tend to zero as hopping distance is larger than $\approx$ 4–5 Å.